The Effective Use of Machine Learning in WorldView-2 Image for the Recognition of Two Forest Species in the Brazilian Atlantic Rainforest

Enzo Luigi Crisigiovanni (enzocrisigiovanni@gmail.com)
Midwestern State University https://orcid.org/0000-0002-5635-3468
Afonso Figueiredo Filho
Universidade Estadual do Centro-Oeste
Vagner Alex Pesck
Universidade Estadual do Centro-Oeste
Vanderlei Aparecido de Lima
Universidade Tecnologica Federal do Parana - Campus Pato Branco

Research

Keywords: Random Forest, Artificial Neural Network, Genetic Algorithm, PHOG, Edge filter, Hovenia dulcis, Araucaria angustifolia

Posted Date: June 10th, 2020

DOI: https://doi.org/10.21203/rs.3.rs-33722/v1

Abstract

Background: Tree species identification by satellite images facilitates the implementation of conservation and forest management measures. However, this recognition is complex in tropical forests, due to the high diversity of spectral responses of existing species, as well as the adjustment of efficient computer vision methods for the process.

Method: In this work we tested the capacity of machine learning algorithms for attribute selection and data mining to recognize crowns of two forest species in the Mixed Rainforest, *Araucaria angustifolia* (Bertol.) Kuntze endangered native species and *Hovenia dulcis* Thunb. an aggressive invasive alien species. For this we used, a fused WordView-2 (2016) image with 0.5 m of spatial resolution. The images of the crowns of the two tree species were cut by photo interpretation, using the compositions 8NIR-2, 3G, 2B and 5R, 3G, 2B. Color and texture descriptors (PHOG and Edge Filter) were applied to the clippings of the images. A genetic algorithm was used to optimize the attribute selection. The species classification was performed by the classifiers: Artificial Neural Networks (ANN) and Random Forest (RF), both bio-inspired algorithms.

Result: The species classification was performed with high accuracy, evidenced by the high hit rate reaching 95% for Cross-Validation. RF surpassed the ANN classification rates and still proved to be more stable and faster for training and executing the algorithm and later species classification. It was concluded that the WorldView-2 multispectral sensor has the potential to provide sufficient information for the recognition of *H. dulcis* and *A. angustifolia* species, contributing to conservation and sustainable maintenance in the Araucaria Forest.

1. Background

The diversity of tree species is an essential variable for the maintenance of terrestrial ecosystems. This is a relevant parameter addressed for the various ecological issues, such as niche modeling, biogeochemical cycles and, therefore, the survey of diversity or the knowledge of certain tree species, becomes increasingly important in sustainable forest management (Wulder et al. 2004; McDermid et al. 2009).

Traditional forest inventories and data acquisition based on field methods are expensive and require a long time to survey the database and require specialized human potential when they are implemented in large areas. In view of these facts, spatial information is of great importance for the management of native forests. Therefore, improved methods such as remote sensing by orbital sensors are necessary to obtain spatial information about the composition of tree species and their distribution patterns in forests and their biomes (Nagendra 2001).

The classification of forest species by images from remote high-resolution sensors has grown a lot in the last ten years. However, this technique only became possible due to the increase in the spatial and example, WordView, Geoeye, Skysat, Pleiades).

Another contributing factor is the ease of using Remotely Piloted Aircrafts (RPAs) with extremely high spatial resolution, but cover a smaller area compared to orbital sensors. These technological devices made it possible to obtain a source of information necessary for the process of classifying forest species by images.

The emergence of machine learning techniques, which makes possible the classification of species, have shown benefits in several fields of technology and science, such as in biology, ecology, physics, chemistry, agronomy, economics, medicine, mathematics and computer science. This was due to its ability to operate with complex calculation issues, which can be applied progressively to solve practical problems. As, for example, we can mention Artificial Neural Network - ANN, one of the most widespread algorithms for matrix classifications, which performs tasks receiving input signals stimulating the network's ability to learn and recognize patterns (Samborska et al. 2014).

Even with all this technological development, the classification process is constantly being improved. Classifications of boreal forests and European Tundra's found excellent results using the Random Forest - RF algorithm in WordView-2 images, reaching a potential for the identification of 20 forest species, with an accuracy of up to 90% (Immitzer et al. 2012).

Given the importance of the identification of forest species by satellite images in forest management programs, this research aimed to explore the capacity of machine learning algorithms Genetic Algorithm - GA, Random Forest - RF, and Artificial Neural Network - ANN, using color and texture descriptors (PHOG and Filter Edge), for the recognition and classification of two forest species present in the Araucaria Forest, *H. dulcis* (invasive alien species) and *A. angustifolia* (endangered native species). Thus, it sought to evaluate the potential of WorldView-2 images to support the classification of these species, in the remote forest inventory.

2. Materials And Methods

2.1 Study Area

In the second plateau of Paraná state, Brazil, located in the central west region can be found a large "continuum" of native Araucaria Forest. This area is preserved by three National Conservation Units (NCU), which cover about 20 km² for research, sustainable management and species preservation, among them *A. angustifolia*. This large area plays an important role in Paraná's water structure, being a watershed in the three large basins of the state Ivaí, Tibagi and Iguaçu. According to the Water and Earth Institute of Paraná (IAT), these three NCUs are areas of relevant ecological interest, being entitled as a strategic area for environmental conservation (IAT 2007).

The present work was carried out in the vicinity of these conservation units, in the Imbituvão sub-basin belonging to the Tibagi basin. The study area is within the rural properties inserted in the project called "Imbituvão", carried out by the Department of Forestry at the Midwestern State University (Fig. 1). This ith a high degree of *H. dulcis* infestation.

This region has a very heterogeneous and fragmented landscape, possibly due to the use and occupation of land by agriculture. Its geological structure consists predominantly of sandstones, whose texture varies from fine to coarse (Salamuni et al. 1969). The predominant types of soil are the red-yellow dystrophic argisol and the nitossol with aluminum oxides (Mazza et al. 2005). The area has a wavy and rugged topography with an average altitude of 800 m and monthly average rainfall close to 200 $mm.month^{-1}$. The climate of the region, according to the Köppen-Geiger classification, is classified as Cfb (temperate), with mild summers, winters with severe and frequent frosts, without a dry season (Maack 2017).

2.2 Study species.

2.2.1 Araucaria angustifolia (Araucaria)

A. angustifolia, known as Araucaria or Paraná Pine is a dominant tree species of the Araucaria Forest. It is an angiosperm conifer, perennial, with unmistakable appearance. It has a trunk, usually single and cylindrical, which can reach an average of 35 m in height and 2.5 m in diameter at breast height at 1.3 m from the ground (DBH). Its crowns are symmetrical and circular in conical shape when young, but as an adult they present a concave crown with average values of 8 m, reaching up to 18 m in diameter. Its pine needles are dark green, simple, alternating, spiral and with a tip ending in a thorn, reaching 6 cm in length by 1 cm wide (Ruiz 2017). This species is also found in isolated forests and in field areas, presenting easy cognitive identification in images of high-resolution remote sensors.

This species is of great importance for the ecosystem in which it is inserted, in the most varied aspects, ecological, economic, historical, social and cultural. However, from the 19th century onwards, this species was intensely exploited for its high economic value, both for logging and for the trade of pine (Andersson 2005). Today its territory is reduced to a minimum fraction, which according to the International Union for the Conservation of Nature and Natural Resources (IUCN) places *A. angustifolia* in Critical Danger of Extinction (Thomas 2013). Recent publications indicate that due to over-exploitation of *A. angustifolia* and climate change, projections for the complete extinction of the species, if conservation measures are not improved, are estimated for 2070 (Wilson et al. 2019).

2.2.2 Hovenia dulcis (Japanese Raisin-tree)

H. dulcis is a deciduous tree species originating in Southeast Asia (China, Japan and Korea), popularly known in Brazil as Japan grape, chicken gut, Japanese cashew, among others. In Brazil it is a species that can reach up to 25 meters in height, with trunks up to 50 cm of DBH and crowns up to 8 m in diameter (Liu et al. 2015). It presents reproductive phases and a very peculiar phenology compared with native species, which also facilitates its cognitive recognition in high resolution images.

This species was introduced in South America, mainly in the southern region of Brazil for ornamental and also forest purposes as the use of wood (Zenni and Ziller 2011). However, due to the similarity of the

raucaria Forest, this species found it easy to

establish and develop in the Southern region of Brazil. The dispersion of this species occurs mainly by medium-sized mammals, such as armadillos (Carvalho 1994), skunks (Cáceres and Monteiro-Filho 2001) and bats (Zortea 1993). Another determining characteristic is the intense production of seeds with high germination rate, especially where there are reductions in litter deposition, indicative of anthropic disturbances in the forest (Dechoum et al. 2015). Due to several favorable factors, there is a strong invasion of *H. dulcis* in the remnants of Araucaria Forest in the South-Central region of Paraná (Figueiredo Filho et al. 2013; Nauiack 2015).

2.3 WorldView-2 satellite

WorldView-2 is a new generation of imager satellites. It is a commercial satellite with passive sensors owned by DigitalGlobe®. It has a heliosynchronous orbit and is approximately 770 km above sea level. It has eight spectral bands 1. Costal Blue (CB: 400–450 nm), 2. Blue (B: 450–510 nm), 3. Green (G: 510–580 nm), 4. Yellow (Y: 585–625 nm), 5. Red (R: 630–690 nm), 6. Red edge (RE: 705–745 nm), 7. Near infrared 1 (NIR-1: 770–895 nm), 8. Near infrared 2 (NIR-2: 860–1040 nm) with spatial resolution of 1.84 m. It also has a panchromatic band of 0.46 m of spatial resolution with a detection interval of 450–800 nm. The satellite sensors have a scene size (coverage of a captured image) of 16.4 km^2, with a radiometric resolution of 11 bits for each pixel. Its temporal resolution is 3.7 days for maximum spatial resolution and 1.1 days with its spatial resolution halved, this off-nadir movement still allows the satellite to produce stereoscopy in the image (DigitalGlobe 2010). The WorldView-2 mission was launched in 2009 and is in operation (providing images) until nowadays.

2.4 Image acquisition and preprocessing

We acquired a WorldView-2 image, captured on 04/30/2016 at 13:42 hours (WV2-2016), with less than 3% cloud cover and covering about 85% of the Imbituvão River sub-basin. The image was orthorectified (WGS 84, UTM – 22S) by the Digital elevation model (DEM) on a scale equivalent to the spatial resolution of the image. In sequence, it was submitted to atmospheric correction, and their radiance values were converted to reflectance by the Fast Line-of-sight Atmospheric Analysis of Spectral Hypercubes (FLAASH) algorithm (Perkins 2012). After atmospheric correction, the image was fused by the Principal components spectral sharpening (PC spectral sharpening) algorithm with resampling based on the nearest neighbor to achieve a spatial resolution of 0.5 m.

2.5 Sample collection and color attributes

Before choosing the area and collecting the samples, a commonly used correlation analysis between bands was performed to adjust functions of the digital values of the pixels. This analysis indicates the similarity between bands; however, the choice of a composition varies according to the application of the image (Inglada 2002). For this work, low similarity values were required in order to add more information in the composition. For the detection of the species *H. dulcis* and *A. angustifolia* the most dissimilar composition was 8NIR-2, 3G, 2B (NIR). After choosing the composition the image was converted from 11 bits to 8 bits. The chosen composition was compared with the natural composition 5R, 3G, 2B (RGB), as

An area of 20 × 20 pixels was used to perform the cutouts of the treetops in the images (sampling). This dimension was defined seeking to cover as much crown area as possible for both species, avoiding pixels that do not correspond to the crowns, or border pixels (such as the remains of the tree itself). The cut-off of isolated hearts was also avoided, thus preventing conflicts in the classification process. Forty-five clippings were made for each species (*A. angustifolia* and *H. dulcis*) and for each RGB and NIR composition, i.e., 90 clippings for each composition. The entire clipping procedure was performed manually by gimp 2.8.22 software with simultaneous image validation of an RPA, with spatial resolution of 0.06 m (eBee - Sensefly®) (Fig. 2).

The 90 clippings of the two species were divided into 2/3 (60 samples) for the construction of classification models and 1/3 (30 samples) for external validation of the models. The choice of cutouts for the construction and validation of the model were made at random and for both RGB and NIR compositions. Each clipping presented an amount of 400 px and each pixel could receive 768 digital values (DN) from each band of the 3×2^{8bits} composition. The distribution of these digital values for each pixel and for each band, are precisely the attributes of color analyzed. The color histograms for each image were extracted by Chemostat software® (Helfer et al. 2015).

2.6 Texture attributes

2.6.1 Pyramid histogram of oriented gradients PHOG

Pyramid is a technique used to reduce the dimensionality of raster-type images, that is, for each step of the pyramid the pixel dimension is halved (for example 20 × 20 px; 10 × 10 px; 5 × 5 px). For this, a weighted average is performed among the closest neighbors, transforming each four pixels of the image into one pixel (Fig. 3A). After reducing the dimensionality of the image, the histogram of oriented gradients (HOG) technique is applied, which is a resource descriptor widely used in computer vision and image processing for object detection purposes (Korom et al. 2014).

The HOG method consists of passing overlapping windows of defined dimensions, in order to scan both horizontally and vertically over the image. This filter pass encodes information about the orientation of the intensity gradients in the image. This coding is performed by vectors oriented in a direction ranging from 0º to 360º degrees (0º, 45º, 90º, 135º, ..., 360º) and intensity based on the digital values of each pixel (Fig. 3A). HOG is a method similar to edge-oriented histograms (or Edge Filters), but it uses local contrast normalization for greater accuracy. Since the discovery of this method, HOG has been applied in different areas of knowledge, including for the detection of forest species by satellite imagery (Dalal and Triggs 2005; Rybski et al. 2010; Hu and Collornosse 2013; Torrione et al. 2014; Jipeng et al. 2020). For this work PHOG and Edge Filter (item 2.6.2) were applied for all samples (cutouts) of both compositions 8NIR-2, 3G, 2B (NIR) and 5R, 3G, 2B (RGB), and for both species *A. angustifolia* and *H. dulcis*.

2.6.2 Edge filter

Edges can be defined as points in a digital image where the brightness of the image changes sharply with [illegible] ...nce of the image changes drastically, are

arranged in a set of segments of lines or curves. Edge detection includes a variety of mathematical methods that aim to identify these discontinuities by brightness changes. This method, like HOG, also consists of passing overlapping dimension windows defined traversing the entire image vertically and horizontally. This image scan identifies borders and organizes them according to their distribution and location (Fig. 3B). This technique has been widely used in computer vision for the detection of objects in an unsupervised manner (Başa 2015), or in the segmentation of images, mainly satellite, for object-oriented classification (Kang et al. 2013). Both texture descriptors (HOG and Edge Filters) were executed by the ImageFilter package implemented in Weka 3.9.3 (Waikato Environment for Knowledge Analysis) (Frank et al. 2016).

2.6.3 Data mining (Genetic algorithm - GA)

Before performing the classification, a data mining technique was used to select the best attributes, for the color histograms and oriented histograms extracted by PHOG (the histograms extracted by Edge Filter did not go through the mining process, because the number of elements extracted by this descriptor were low). For such mining, the Genetic Algorithm – GA was used, which is a metaheuristic bioinspired by the adaptive process of natural selection, and thus uses operators such as crossover and mutation to select the best attributes in a data set (Huang and Wang 2006). GA belongs to the larger class of evolutionary algorithms (EA) and are commonly used to generate high-quality solutions to optimization problems in operational surveys, but has been widely applied for the detection of objects in remote sensor images (Bhanu et al. 1995; Celik 2010; Hashemi et al. 2010; Xu et al. 2020).

For this context of selection of better color and texture attributes of the images, the GA was adjusted with the following hyperparameters: 60% probability of crossover and 3.3% of mutation. The crossings occurred with a maximum population of 20 individuals with selection time of 20 generations. This algorithm was applied to the 60 separate individuals for the construction of classification models. Figure 4 details the input of the attributes of the clippings of each image to be selected by the GA algorithm.

2.7 Classification algorithms: Artificial Neural Network - ANN and Random forest - RF

After choosing the best attributes for both compositions by GA, both for color and texture attributes, two classification algorithms were applied: 1) Artificial Neural Network – ANN and 2) Random forest – RF. Both classification algorithms were performed with cross validation by the K-folds 10/90 method (Fig. 5). The classification was also validated by the Kappa index, which evaluates the agreement of the data sets classified by the classification algorithm. Machine learning algorithms were also run by Weka 3.9.3 software.

2.7.1 Multilayer Perceptron (MLP)

The MLP algorithm is also a bioinspired algorithm based on the functioning of human neuron layers

er of input neurons and a hidden output layer.

The impulses received by the dendrites represent the data entry in the algorithm, which in this case were the attributes of texture and color. The ANN classification process is performed by iterations called epochs; between each epoch there may be adjustments in the weights assigned to the input data, modifying the paths made between neurons of the network for classification. These adjustments represent the learning rate of the algorithm, which for this case was used a learning rate of 0.3, with variation of training time epochs from 0 to 500.

2.7.2 Random Forest (RF)

RF is also a bioinspired algorithm, but based on decision trees. This algorithm builds a new database based on the original by classifying the two databases into original and artificial. The algorithm then performs a sequence of decision trees, and instead of searching for the most important resource when splitting a node, it looks for the best resource among a random subset of resources (a forest of decision trees, Fig. 5) (Breiman 2001). For this case, the hyperparameters were 100 decision trees to be analyzed in 100 search iterations.

2.8 Accuracy analysis

For the verification of the classification capacity of the RF and ANN algorithms, percentages of correct answers were used for both species in relation to the total number of cutouts classified by the model. Together with the Kappa index (Eq. 1), which has been extensively used to analyze the accuracy of classifier algorithms (Sasikala et al. 2017). This index recorded the number of correct and false positives classified by the algorithm, for both species *H. dulcis* and *A. angustifolia*. Its equation is given by:

$$K = \frac{\sum_{i=1}^{C} \frac{x_{ij}}{n} - \sum_{i=1}^{C} \frac{x_i * x_j}{n}}{1 - \sum_{i=1}^{C} \frac{x_i * x_j}{n}} \quad (1)$$

Where: x_{ij} = value in row i and column; x_i = sum of the line i; x_j = sum of the column *j* of the confusion matrix; *n* = total number of samples; *c* = total number of classes.

3. Results

3.1 Color and texture attributes selection

The extraction of color attributes was performed by the reflectance histogram of the image clippings. Fig 6 shows that the reflection patterns for each of the RGB and NIR bands are very peculiar for both *H. dulcis* and *A. angustifolia*. It can be observed that the shade of green reflected by *A. angustifolia* is darker than *H. dulcis*. Regarding the amplitude of the reflected gray levels, we can observe that *A. angustifolia* reflectance interval is about 50 shades of gray darker than *H. dulcis*. It is also remarkable the greater dispersion of the values reflected in the infrared range to *H. dulcis.*

Attributes extraction by texture descriptors was also performed based on the reflectance values of Fig 6. However, texture descriptors take into account the position of each pixel in order to find discontinuities or sudden changes in reflection patterns. The attributes selected by PHOG are based on the size of the image and the number of pyramids performed to reduce the dimensionality of the image. Thus, the number of attributes selected for the different compositions and different species was 630 attributes in total. For the Edge Filter, the results were different, since different numbers of attributes per species are extracted. For the Edge Filter, the compositions of the RGB and NIR images were 80 attributes selected in total.

The genetic search algorithm, with the hyperparameters proposed in the literature, was able to reduce by about 60% the amount of input data for the classifier algorithms. With the use of GA, we obtained optimization rates of up to 10%, comparing with and without the use of GA, for RF and ANN classifiers. This reduction can be observed both for color histograms and for the attributes selected by the texture descriptor PHOG.

3.2 RF and ANN classifiers

Both RF and ANN classifiers showed high performance, with high and similar classification rates, as we can see in Figure 7A. However, RF showed greater accuracy for both the color attributes and the attributes of the two texture descriptors. An average increase of 2.5% was observed, corresponding to two additional images correctly classified by RF in Cross-Validation (CV). The addition of correct classifications for external validation (VE) was 6.4% using RF as a classifier. When all instances (all images) (MOD) were used, the increase was 0.28%, practically null (Table 1).

When comparing the two compositions (RGB and NIR), considering both color and texture descriptors, we can observe that in short there was a better classification for the NIR composition of the images, in relation to RGB (Fig 7B). Analyzing ANN there was an increase of 11.6% for using CV, 2.3% for EV and 11.1% for MOD. With regard to RF, there was still a greater contrast between the compositions, with an increase of 12.2% for the CV, 8.9% for the VE and 10.6% for the MOD (Table 1).

Focusing on the correct percentage of images classified by species by both algorithms, we can observe that there were no major difficulties for both RF and ANN in classifying species for color descriptors (Fig 7). For RGB images (color images) there was a higher rate of classification of *H. dulcis* with a difference of 2.3% in CV in relation to *A. angustifolia*. This increase was maintained, however in a subtle way, showing an increase of 0.83% for the MOD. In contrast, for the VE, *A. angustifo*lia stood out with an increase of 6.7% of correct classification in relation to the species *H. dulcis* (Table 1).

However, this scenario was completely different with respect to texture descriptors (PHOG and Edge Filter). For this case, all the results for *A. angustifolia* outweighed the values of the classifications, demonstrating that the texture descriptors for the recognition of *H. dulcis* were not as efficient as for *A.* [illegible] rates in relation to *A. angustifolia* was

25.42% lower for CV (equivalent for this case, 7 individuals classified incorrectly), 20% lower for EV (6 individuals) and 15.83% lower for MOD (4 individuals), respectively (Table 1).

We can observe that when we classify the images by the texture descriptors PHOG and Edge Filter (Fig 9 and Table 1), the differences in classifications between species show greater contrast. The classification of *H. dulcis* for texture was low, mainly due to PHOG attributes. On the other hand, for *A. angustifolia*, the scenario reverses, with subtle variations in the classification. The PHOG descriptors for *A. angustifolia* proved to be better, when classified by RF and ANN. Cross-validation (CV) was over 99%, well above the CV for *H. dulcis*.

Since the classification of *H. dulcis* using PHOG did not obtain high rates, we can better analyze the results, comparing the differences in the accuracy of PHOG between the NIR and RGB compositions (Table 1). The reduction in the percentage of *H. dulcis* classification was due to RGB composition, that is, the extraction of attributes by PHOG for this species, was not efficient, both for RF and ANN. Kappa: CV: 0.23, VE: 0.07 and MOD: 0.37.

COLOUR ATRIBUTES							
ANN-RBG	Kappa	*a*	*b*	classified as	Classification		
CV	0.87	27	3	*a = A. angustifolia*	Correctly	56	93.3%
		1	29	*b = H. dulcis*	Incorrectly	4	6.7%
EV	0.93	14	1	*a = A. angustifolia*	Correctly	29	96.7%
		0	15	*b = H. dulcis*	Incorrectly	1	3.3%
MOD	0.97	29	1	*a = A. angustifolia*	Correctly	59	98.3%
		0	30	*b = H. dulcis*	Incorrectly	1	1.7%
RF-RBG							
CV	0.90	28	2	*a = A. angustifolia*	Correctly	57	95.0%
		1	29	*b = H. dulcis*	Incorrectly	3	5.0%
EV	1.00	15	0	*a = A. angustifolia*	Correctly	30	100.0%
		0	15	*b = H. dulcis*	Incorrectly	0	0.0%
MOD	1.00	30	0	*a = A. angustifolia*	Correctly	60	100.0%
		0	30	*b = H. dulcis*	Incorrectly	0	0.0%
ANN-NIR							
CV	0.87	28	2	*a = A. angustifolia*	Correctly	56	93.3%
		2	28	*b = H. dulcis*	Incorrectly	4	6.7%
EV	0.73	14	1	*a = A. angustifolia*	Correctly	26	86.7%
		3	12	*b = H. dulcis*	Incorrectly	4	13.3%
MOD	1.00	30	0	*a = A. angustifolia*	Correctly	60	100.0%
		0	30	*b = H. dulcis*	Incorrectly	0	0.0%
RF-NIR							
CV	0.90	28	2	*a = A. angustifolia*	Correctly	57	95.0%
		1	29	*b = H. dulcis*	Incorrectly	3	5.0%
EV	0.80	15	0	*a = A. angustifolia*	Correctly	27	90.0%
		3	12	*b = H. dulcis*	Incorrectly	3	10.0%
MOD	1.00	30	0	*a = A. angustifolia*	Correctly	60	100.0%
		0	30	*b = H. dulcis*	Incorrectly	0	0.0%

TEXTURE ATRIBUTES							
ANN-RBG PHOG							
CV	0.23	30	0	*a = A. angustifolia*	Correctly	37	61.7%
		23	7	*b = H. dulcis*	Incorrectly	23	38.3%
EV	0.07	14	1	*a = A. angustifolia*	Correctly	16	53.3%
		13	2	*b = H. dulcis*	Incorrectly	14	46.6%
MOD	0.37	30	0	*a = A. angustifolia*	Correctly	41	68.3%
		19	11	*b = H. dulcis*	Incorrectly	19	31.7%
RF-RBG PHOG							
CV	0.23	30	0	*a = A. angustifolia*	Correctly	37	61.7%
		23	7	*b = H. dulcis*	Incorrectly	23	38.3%
EV	0.07	14	1	*a = A. angustifolia*	Correctly	16	53.3%
		13	2	*b = H. dulcis*	Incorrectly	14	46.7%
MOD	0.37	30	0	*a = A. angustifolia*	Correctly	60	68.3%
		19	11	*b = H. dulcis*	Incorrectly	0	31.7%
ANN-NIR PHOG							
CV	0.83	30	0	*a = A. angustifolia*	Correctly	55	91.7%
		5	25	*b = H. dulcis*	Incorrectly	5	8.3%
EV	0.53	14	1	*a = A. angustifolia*	Correctly	23	76.7%
		6	9	*b = H. dulcis*	Incorrectly	7	23.3%
MOD	1.00	30	0	*a = A. angustifolia*	Correctly	60	100.0%
		0	30	*b = H. dulcis*	Incorrectly	0	0.0%
RF-NIR PHOG							
CV	0.90	29	1	*a = A. angustifolia*	Correctly	57	95.0%
		2	28	*b = H. dulcis*	Incorrectly	3	5.0%
EV	0.80	14	1	*a = A. angustifolia*	Correctly	27	90.0%
		2	13	*b = H. dulcis*	Incorrectly	3	10.0%
MOD	1.00	30	0	*a = A. angustifolia*	Correctly	60	100.0%

		0	30	*b = H. dulcis*	Incorrectly	0	0.0%
ANN-RBG Edge							
CV	0.50	24	6	*a = A. angustifolia*	Correctly	45	75.0%
		9	21	*b = H. dulcis*	Incorrectly	15	25.0%
EV	0.53	12	3	*a = A. angustifolia*	Correctly	23	76.7%
		4	11	*b = H. dulcis*	Incorrectly	7	23.3%
MOD	1.00	30	0	*a = A. angustifolia*	Correctly	60	100.0%
		0	30	*b = H. dulcis*	Incorrectly	0	0.0%
RF-RBG Edge							
CV	0.60	24	6	*a = A. angustifolia*	Correctly	48	80.0%
		6	24	*b = H. dulcis*	Incorrectly	12	20.0%
EV	0.67	14	1	*a = A. angustifolia*	Correctly	25	83.3%
		4	11	*b = H. dulcis*	Incorrectly	5	16.7%
MOD	1.00	30	0	*a = A. angustifolia*	Correctly	60	100.0%
		0	30	*b = H. dulcis*	Incorrectly	0	0.0%
ANN-NIR Edge							
CV	0.60	27	3	*a = A. angustifolia*	Correctly	48	80.0%
		9	21	*b = H. dulcis*	Incorrectly	12	20.0%
EV	0.40	10	5	*a = A. angustifolia*	Correctly	21	70.0%
		4	11	*b = H. dulcis*	Incorrectly	9	30.0%
MOD	1.00	30	0	*a = A. angustifolia*	Correctly	60	100.0%
		0	30	*b = H. dulcis*	Incorrectly	0	0.0%
RF-NIR Edge							
CV	0.67	25	5	*a = A. angustifolia*	Correctly	50	83.3%
		5	25	*b = H. dulcis*	Incorrectly	10	16.7%
EV	0.67	13	2	*a = A. angustifolia*	Correctly	25	83.3%
		3	12	*b = H. dulcis*	Incorrectly	5	16.7%
MOD	1.00	30	0	*a = A. angustifolia*	Correctly	60	100.0%
		0	30	*b = H. dulcis*	Incorrectly	0	0.0%

Legend: CV Cross-Validation; EV External validation and MOD using the supplied test set (all instances).

Table 1
Kappa index and the correct answers percentage of classifiers, compositions and descriptors.

The computational time spent for the construction and training of the models was also analyzed. The computational effort spent to run the RF algorithm was about 10 times lower than for the ANN algorithm (data not shown). When analyzing the recognition rate by the ANN classifier in relation to the number of epochs that the algorithm processes, we can notice that with 500 times, the network system stabilizes for both image compositions, RGB and NIR. The learning of the neural network by its percentage of classification (Cross-validation) as a function of epochs was plotted (Fig 10A and 10B). Another factor that can be emphasized is the need for a larger number of epochs for the curve to achieve an asymptotic behavior when texture attributes are used, when compared with color attributes by the RGB channels. We can observe that, 100 epochs, the neural network could already be trained, without loss of quality in the classification and with much lower computational cost, compared to when using 500 times. It can also be noted that the inflection points of the curves, that is, the moments where there is the highest classification with the shortest possible time (obtained by the first derivative of the function), happens in the first 10 iterations.

4. Discussion

The results revealed the recognition potential of *H. dulcis* and *A. angustifolia* by RF and ANN in WorldView-2 Image. These results come from a series of geoprocessing and computer vision methodologies implemented in the present work. First, we can mention the sample design referring to the collection of the cutouts of the crowns of the two tree species. This collection was performed in such a way that the sampled individuals presented the same crowns shape pattern and a homogeneous distribution along the image, avoiding overlapping of crowns, trees in edge or isolated conditions (Fig. 1). Also, as a collection criterion, the detailed choice of representative individuals (healthy trees with similar crowns sizes and shapes) was performed. This selection of individuals was only possible by confirming the individuals sampled by RPA-type imaging sensors.

Another decisive factor addressed in this work was the choice of the dimension of clipping of the images for both species. Researchers with similar aim of the present study, sought to detect the invasive species *Solanum mauritianum* in South Africa (native species of the Brazilian Atlantic forest), also in WorldView-2 images with RF as a classifier (Peerbhay et al. 2016). They obtained dimensions of optimal clippings between 15 and 17 m², an average of 16 × 16 px for the fused image. Thus, the choice of an average value of 20 × 20 px for larger species such as *H. dulcis* and *A. angustifolia* proved promising and can be used in the future as a scale parameter for segmentation in object-oriented classifications.

H. dulcis presents a phenology and reproductive cycles very expressive and delimited. In southern Brazil, this species blooms from August to February and has ripe fruits from March to October. There is also a total leaf loss season that runs from April/May to August, and at the end of August regrowth begins (Carvalho 1994). These phenological characteristics can be easily observed, cognitively, in high-resolution satellite images, except for the months of February to April, when the foliage presents a shade of green similar to the other Araucaria Forest leaf-species. The species *A. angustifolia* does not present changes during the year, but because it is one of the highest species of the Atlantic forest and by the characteristics of the pine needle, its detection in images is also facilitated.

These phenological differences between the two species were taken into account to be compared by color and texture descriptors. It was expected, a priori, that due to the date of capture of the scene (04/30/2016) at the beginning of the flowering of *H. dulcis*, a phase by which the species still meets the shade of green similar to the other leafy species the color attributes were not so significant. However, these proved to be more efficient for the distinction of species, mainly related to the classification of *H. dulcis.* This result indicates that even near times when *H. dulcis* does not stand out visually, the species presents a high contrast between the rates of reflection in relation to *A. angustifolia*. This differentiation was even greater when the attributes were analyzed by the composition with the infrared band (NIR-2). On the other hand, the textural descriptors demonstrate a higher efficiency (for both classifiers) in the detection of *A. angustifolia*, a result that is in favor of the expected a priori. These results are mainly due to the singular shape of their crowns, which present numerous discontinuities of edges by the different shadings formed by the shape of the branches.

In summary, we found high rates of correct classifications for both species, by the classification algorithms, RF and ANN. Still, we observed that there was low computational processing cost to run the algorithms. However, the highest recognition values were achieved by the RF classifier to the detriment of ANN, which in addition to obtaining lower classification rates required a higher computational cost for network training. There are studies that point to greater stability and predictive power of ANN with respect to RF when adjusted regression models for optimization purposes (Ahmad et al. 2017). However, there are several studies indicating that the RF classifier achieves better classification results when applied to data from multispectral satellite images, besides requiring configurations with fewer hyperparameters for the adjustment of its models (Chan et al. 2012; Shao et al. 2015).

Some characteristics presented of the efficient application of RF with multispectral images for classifications of different tree species could be shown in this work. It was evident the increase in the correct classification rates for both species, when the NIR composition was used. This fact indicates the importance of gaining spectral information when using quality data from sensors such as WorldView-2.

Another characteristic of RF is its greater stability, regarding the number and size of samples used for training when compared to other classifiers. This is due to the large number of decision trees produced by randomly selecting a subset of training samples and a subset of variables to split each node in the tree. Comparisons published using RF and other group classifiers such as AdaBoost reported that both

classifiers produced similar classification results, however the RF algorithm showed greater speed to train the data and greater stability in the classification (Chan and Paelinckx 2008; Miao et al. 2012).

5. Conclusion

This study demonstrated that the WorldView-2 multispectral sensor has the potential to provide sufficient information for the recognition of the species *H. dulcis* and *A. angustifolia* in the Araucaria Forest. The RF and ANN machine learning algorithms were effective for classifying these species, reaching close to 95%. This result was possible to be achieved due to the choice of the sample design with scale factors for sample collection and the use of color and texture descriptors (PHOG and Edge Filter). Color attributes, mainly related to infrared band (NIR-2), were more efficient for classification compared to texture attributes. Regarding texture, the classification of *H. dulcis* was not satisfactory, but the attributes extracted by the Edge Filter were efficient in the classification of *A. angustifolia.* Furthermore, data mining by genetic algorithm indicated that by selecting the best attributes, it reduced the size of the data entry and increased the performance of the RF and ANN classifiers.

Additional studies covering different types of vegetation in different phytogeographic contexts and periods of the year (spatiotemporal) are needed to confirm the potential of WorldView-2 data to be used for classification of these species. Therefore, other species of the Araucaria Forest should also be evaluated in order to increase the diversity of spectral responses and improve the remote forest inventory.

We can conclude that the sample design, the use of WorldView-2 sensor images, the choice of descriptors and GA, RF and ANN algorithms were efficient for the classification of the species addressed here. This work contributes to improvements in the methods of recognition and identification of tree species by high resolution image and by computer vision. Consequently, provides information that contributes to conservation and management of the Araucaria Forest, considering that *A. angustifolia* is the characteristic and dominant species of this forest typology, contrasting with *H. dulcis*, a worrying and aggressive invasive alien species.

Abbreviations

NCU: National Conservation Units; IAT: Instituto Água e Terra (Brazilian environmental agency); DBH: Diameter at breast height; IUCN: Union for the Conservation of Nature and Natural Resources; DEM: Digital elevation model; WGS: World Geodetic System; UTM: Universal Transverse of Mercator; WV2: WorldView2 (satellite); RPA: Remotely Piloted Aircraft; ANN: Artificial Neural Network; MLP: Multilayer Perceptron (neural network architecture); RF: Random Forest; PHOG: Pyramid Histogram of Oriented Gradients; GA: Genetic Algorithm; R: Red; G: Green; B: Blue; NIR: Near infrared; CV: Cross-Validation; EV: External validation; MOD: Model using the supplied test set (all instances).

Declarations

Ethics approval and consent to participate

The work does not involve any ethical risks

Consent for publication

Not applicable

Availability of data and material

The datasets used during the current work are available from the corresponding author on request.

Competing interests

The authors state that do not have any competing financial interests that could compromise the integrity of the work.

Funding

National Council for Scientific and Technological Development of Brazil (CNPq) and Coordination for the Improvement of Higher Education Personnel of Brazil (CAPES).

Authors' contributions

Crisigiovanni E. L. designed the methods, realized the experiments, processed the data, analyzed the results and wrote the majority of the manuscript. Figueiredo Filho A. idealized the article, provide the materials (satellite image), formulated the research framework. Pesck V. A. contributed in the geoprocessing and remote sensing analysis and cooperated in the design of the methodology. Lima de V. A. cooperated in the methodology design, realized the machine learning analyses and data processing. All authors participated of the manuscript writing, review and edition since the first version the same way have read and approved the final manuscript.

Acknowledgements

The authors would like to thank the Imbituvão project, funded by National Council for Scientific and Technological Development of Brazil (CNPq) and for the technical cooperation between the State Secretariat of Science Technology and Higher Education (SETI) and the Ministry for Science, Research and Arts of Baden-Württemberg for the availability of the WorldView-2 image. We are also grateful to

Coordination for the Improvement of Higher Education Personnel of Brazil (CAPES) for the financial support for the work development.

References

1. Ahmad MW, Mourshed M, Rezgui Y (2017) Trees vs Neurons: Comparison between random forest and ANN for high-resolution prediction of building energy consumption. Energy Build 147:77–89. https://doi.org/10.1016/j.enbuild.2017.04.038.
2. Andersson FA (2005) Coniferous Forests. Elsevier, pp. 296-297.
3. Başa B (2015) Implementation of Hog Edge Detection Algorithm Onfpga's. Procedia - Soc Behav Sci 174:1567–1575. https://doi.org/10.1016/j.sbspro.2015.01.806.
4. Bhanu B, Lee S, Ming J (1995) Adaptative image segmentation using Genetic Algorithm. IEEE Trans Syst man, Cybern 25:1543–1567. https://doi.org/10.1109/21.478442.
5. Breiman L (2001) Random forests. Mach Learn 5–32. https://doi.org/doi:10.1023/a:1010933404324.
6. Cáceres NC, Monteiro-Filho ELA (2001) Food Habits, Home Range and Activity of *Didelphis aurita* (Mammalia, Marsupialia) in a Forest Fragment of Southern Brazil. Stud Neotrop Fauna Environ 36:85–92. https://doi.org/10.1076/snfe.36.2.85.2138.
7. Carvalho PER (1994) Ecologia, silvicultura e usos da uva-do-Japão (*Hovenia dulcis* Thunberg). Embrapa Florestas-Circular Técnica 23:24.
8. Celik T (2010) Change detection in satellite images using a genetic algorithm approach. IEEE Geosci Remote Sens Lett 7:386–390. https://doi.org/10.1109/LGRS.2009.2037024.
9. Chan JCW, Beckers P, Spanhove T, Borre J Vanden (2012) An evaluation of ensemble classifiers for mapping Natura 2000 heathland in Belgium using spaceborne angular hyperspectral (CHRIS/Proba) imagery. Int J Appl Earth Obs Geoinf 18:13–22. https://doi.org/10.1016/j.jag.2012.01.002.
10. Chan JCW, Paelinckx D (2008) Evaluation of Random Forest and Adaboost tree-based ensemble classification and spectral band selection for ecotope mapping using airborne hyperspectral imagery. Remote Sens Environ 112:2999–3011. https://doi.org/10.1016/j.rse.2008.02.011.
11. Dalal N, Triggs B (2005) Histograms of Oriented Gradients for Human Detection. In: Proceedings of the 2005 IEEE Computer Society Conference on Computer Vision and Pattern Recognition (CVPR'05). pp 886–893
12. Dechoum M de S, Rejmánek M, Castellani TT, Zalba SM (2015) Limited seed dispersal may explain differences in forest colonization by the Japanese raisin tree (*Hovenia dulcis* thunb.), an invasive alien tree in southern Brazil. Trop Conserv Sci 8:610–622. https://doi.org/10.1177/194008291500800303.
13. DigitalGlobe (2010) The Benefits of the Eight Spectral Bands, p 12.
14. Figueiredo Filho A., Nauiack CHB., Roik M., Gomes GS (2013) Inventário das florestas nativas em , Centro-Sul do Paraná. 1:115.

15. Frank E, Hall MA, Witten IH (2016) The WEKA Workbench. Online Appendix. In: Data Mining: Practical Machine Learning Tools and Techniques, 4th edn.
16. Hashemi S, Kiani S, Noroozi N, Moghaddam ME (2010) An image contrast enhancement method based on genetic algorithm. Pattern Recognit Lett 31:1816–1824. https://doi.org/10.1016/j.patrec.2009.12.006.
17. Helfer GA, Bock F, Marder L, et al (2015) Chemostat, um software gratuito para análise exploratória de dados multivariados. Quim Nova 38:575–579. https://doi.org/http://dx.doi.org/10.5935/0100-4042.20150063.
18. Hu R, Collornosse J (2013) A performance evaluation of gradient field HOG descriptor for sketch based image retrieval. Comput Vis Image Underst 117:790–806. https://doi.org/10.1016/j.cviu.2013.02.005.
19. Huang CL, Wang CJ (2006) A GA-based feature selection and parameters optimizationfor support vector machines. Expert Syst Appl 31:231–240. https://doi.org/10.1016/j.eswa.2005.09.024.
20. IAT (2007) Refinamento das Áreas Prioritárias para a Conservação da Biodiversidade no Paraná. Curitiba.
21. Immitzer M, Atzberger C, Koukal T (2012) Tree Species Classification with Random Forest Using Very High Spatial Resolution 8-Band WorldView-2 Satellite Data. 2661–2693. https://doi.org/10.3390/rs4092661.
22. Inglada J (2002) Similarity measures for multisensor remote sensing images. Int Geosci Remote Sens Symp 1:104–106. https://doi.org/10.1109/igarss.2002.1024955.
23. Jipeng T, Manasa S, Manjunath TC (2020) An Optimized Method Using CNN , RF , Cuckoo Search and HOG for Early Detection of Eye Disease in Humans. 4:2–5. https://doi.org/http://dx.doi.org/10.24018/ejece.2020.4.2.202.
24. Korom A, Phua MH, Hirata Y, Matsuura T (2014) Extracting oil palm crown from WorldView-2 satellite image. IOP Conf Ser Earth Environ Sci 18:. https://doi.org/10.1088/1755-1315/18/1/012044.
25. Liu T, Hua S, Wang Z (2015) Dietary Chinese Herbs. Diet Chinese Herbs 417–423. https://doi.org/10.1007/978-3-211-99448-1.
26. Maack R (2017) Geografia física do estado do Paraná, 4th edn. Editora UEPG, Ponta Grossa.
27. Mazza CA da S, Santos JE dos, Mazza MCM, et al (2005) Caracterização Ambiental dos Componentes Estruturais da Paisagem do Município de Irati, Paraná, 1st edn. Empresa Brasileira de Pesquisa Agropecuária Embrapa Florestas, Colombo.
28. McDermid GJ, Hall RJ, Sanchez-Azofeifa GA, et al (2009) Remote sensing and forest inventory for wildlife habitat assessment. For Ecol Manage 257:2262–2269. https://doi.org/10.1016/j.foreco.2009.03.005.
29. Miao X, Heaton JS, Zheng S, et al (2012) Applying tree-based ensemble algorithms to the classification of ecological zones using multi-temporal multi-source remote-sensing data. Int J Remote Sens 33:1823–1849. https://doi.org/10.1080/01431161.2011.602651.

30. Nagendra H (2001) Using remote sensing to assess biodiversity. Int J Remote Sens 22:2377–2400. https://doi.org/10.1080/01431160117096.
31. Nauiack CH (2015) Regimes de manejo para *Hovenia dulcis* Thunb. em Floresta Ombrófila Mista como alternativa de controle e geração de rendas. Dissertation, Midwestern State University.
32. Peerbhay K, Mutanga O, Lottering R, Ismail R (2016) Mapping *Solanum mauritianum* plant invasions using WorldView-2 imagery and unsupervised random forests. Remote Sens Environ 182:39–48. https://doi.org/10.1016/j.rse.2016.04.025.
33. Perkins T (2012) Speed and accuracy improvements in FLAASH atmospheric correction of hyperspectral imagery. Opt Eng 51:111707. https://doi.org/10.1117/1.oe.51.11.111707.
34. Ruiz ECZ (2017) Biomassa e flora epifítica de copas de *Araucaria angustifolia*. Dissertation, Midwestern State University.
35. Rybski PE, Huber D, Morris DD, Hoffman R (2010) Visual classification of coarse vehicle orientation using Histogram of Oriented Gradients features. 1–6. https://doi.org/doi:10.1109/ivs.2010.5547996.
36. Salamuni R, Hertel R, Silva J (1969) História do Paraná, 2nd edn. Grafipar, Curitiba.
37. Samborska IA, Alexandrov V, Sieczko L, Kornatowska B (2014) Signpost Open Access Journal of NanoPhotoBioSciences Artificial neural networks and their application in biological and agricultural research. 02:14–30.
38. Sasikala BS, Biju VG, Prashanth CM (2017) Kappa and accuracy evaluations of machine learning classifiers. RTEICT 2017 - 2nd IEEE Int Conf Recent Trends Electron Inf Commun Technol Proc 2018-Janua:20–23. https://doi.org/10.1109/RTEICT.2017.8256551.
39. Shao Y, Campbell JB, Taff GN, Zheng B (2015) An analysis of cropland mask choice and ancillary data for annual corn yield forecasting using MODIS data. Int J Appl Earth Obs Geoinf 38:78–87. https://doi.org/10.1016/j.jag.2014.12.017.
40. Tang J, Deng C, Huang GB (2016) Extreme Learning Machine for Multilayer Perceptron. Lyon Chir 27:809–821. https://doi.org/doi:10.1109/tnnls.2015.2424995.
41. Thomas P (2013) *Araucaria angustifolia*. IUCN Red List Threat Species 2013. https://doi.org/http://dx.doi.org/10.2305/IUCN.UK.2013-1.RLTS.T32975A2829141.en.
42. Torrione PA, Morton KD, Sakaguchi R, Collins LM (2014) Histograms of oriented gradients for landmine detection in ground-penetrating radar data. IEEE Trans Geosci Remote Sens 52:1539–1550. https://doi.org/10.1109/TGRS.2013.2252016.
43. Wilson OJ, Walters RJ, Mayle FE, et al (2019) Cold spot microrefugia hold the key to survival for Brazil's Critically Endangered Araucaria tree. Glob Chang Biol 25:4339–4351. https://doi.org/10.1111/gcb.14755.
44. Wulder MA, Hall RJ, Coops NC, Franklin SE (2004) High Spatial Resolution Remotely Sensed Data for Ecosystem Characterization. Bioscience 54:511. https://doi.org/10.1641/0006-3568.
45. Xu K, Chen E, Li Z, et al (2020) An automatic optimization method of forest type classification using PolSAR image based on genetic algorithm. 2019 6th Asia-Pacific Conf Synth Aperture Radar 1–5.

https://doi.org/10.1109/apsar46974.2019.9048333.

46. Zenni RD, Ziller RS (2011) Visao geral das plantas exoticas invasoras no Brasil. Rev Bras Bot 34:431–446. https://doi.org/10.1590/S0100-84042011000300016.

47. Zortea M (1993) Folivory in *Platyrrhinus (Vampyrops) lineatus*. Bat Res News 34:59–60.

Figures

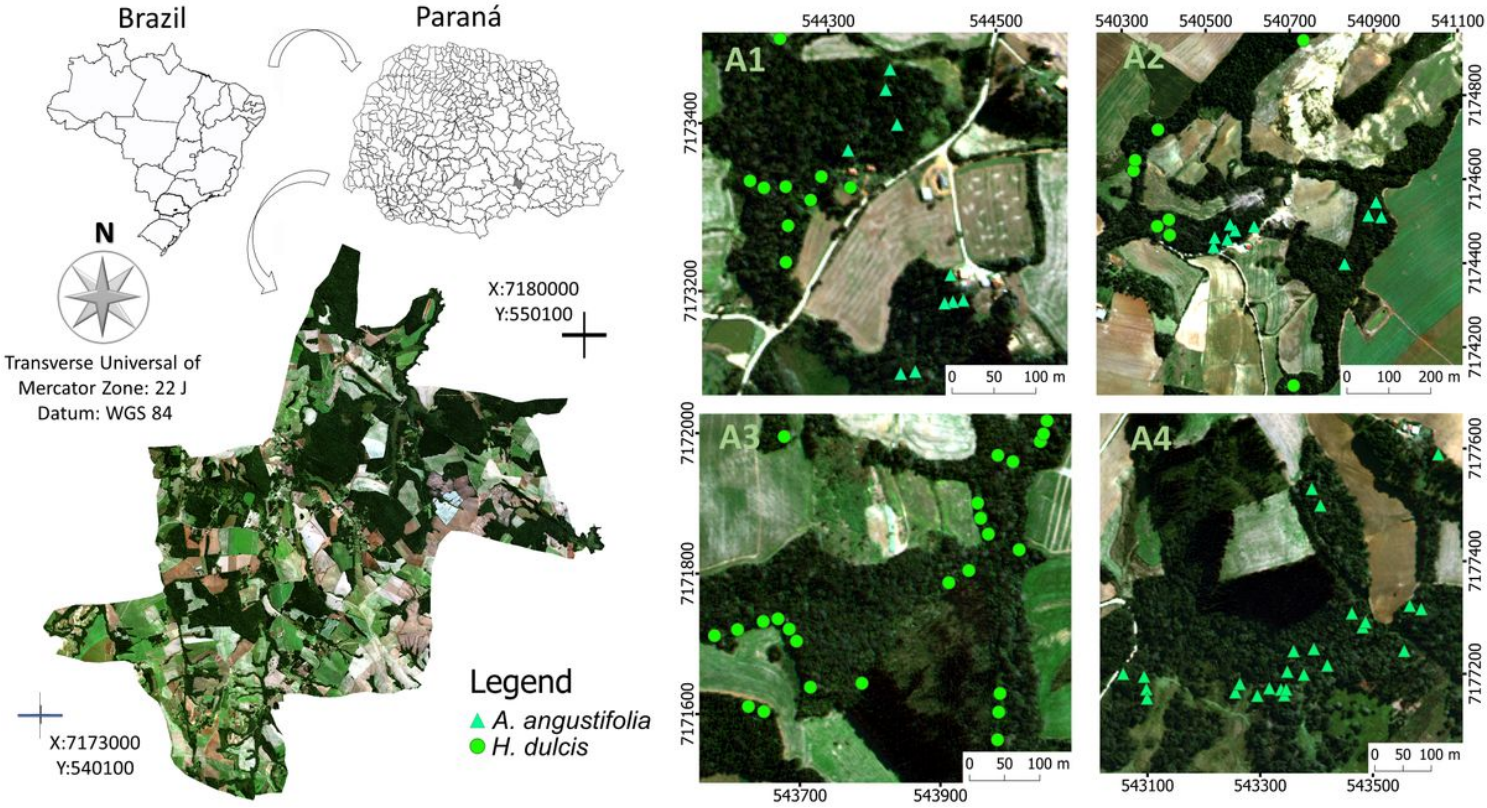

Figure 1

Location of the study and the four properties where the sampling was carried out. Legend: On the left is the geographical location of the project area in the sub-basin of the Imbituvão. On the right are the four rural properties (A1, A2, A3 and A4), with the spatial location of the sample units (crowns of A. angustifolia and H. dulcis), via manual image clipping WorldView-2.

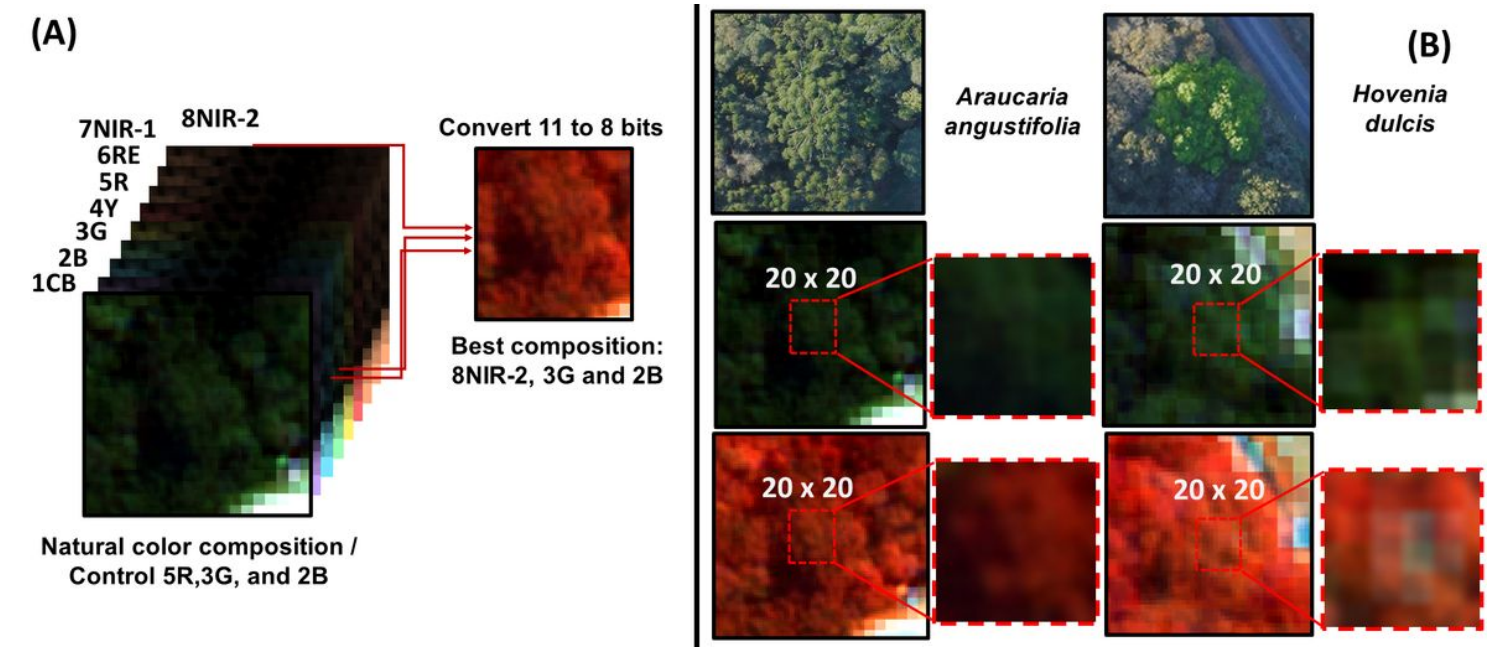

Figure 2

Spectral-bands correlation, radiometric conversion and sample collection by crowns clipping of A. angustifolia and H. dulcis. Legend: (A) Correlation between the 8 spectral bands of the WorldView-2 sensor, choice of compositions 8NIR-2, 3G, 2B (NIR) and 5R, 3G, 2B (RGB) and radiometric conversion. (B) Collection of samples by clipping 20 x 20px the crowns of A. angustifolia and H. dulcis in both compositions, in simultaneous confirmation with the RPA's images.

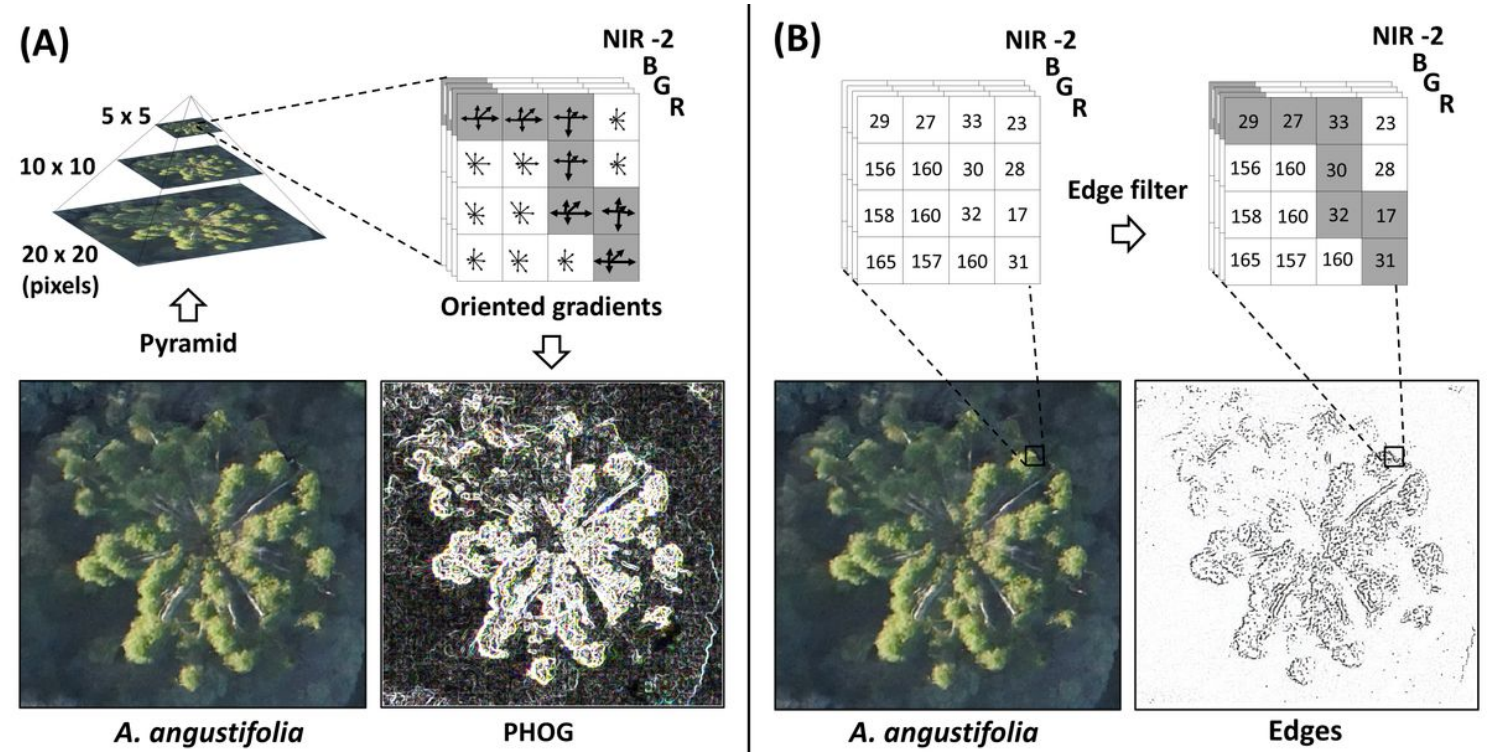

Figure 3

Process of obtaining texture attributes by PHOG and Edge Filter descriptors. Legend: (A) PHOG, reduction of the dimensionality of the crown's cutout followed by the application of the histogram of oriented gradients, by scanning the image by windows. (B) Application of Edge Filter for detection of discontinuities in pixel values. Both images of A. angustifolia in (A and B) come from the RPA used in the work and were posted in Fig 3 to facilitate the visualization of texture attributes extraction process).

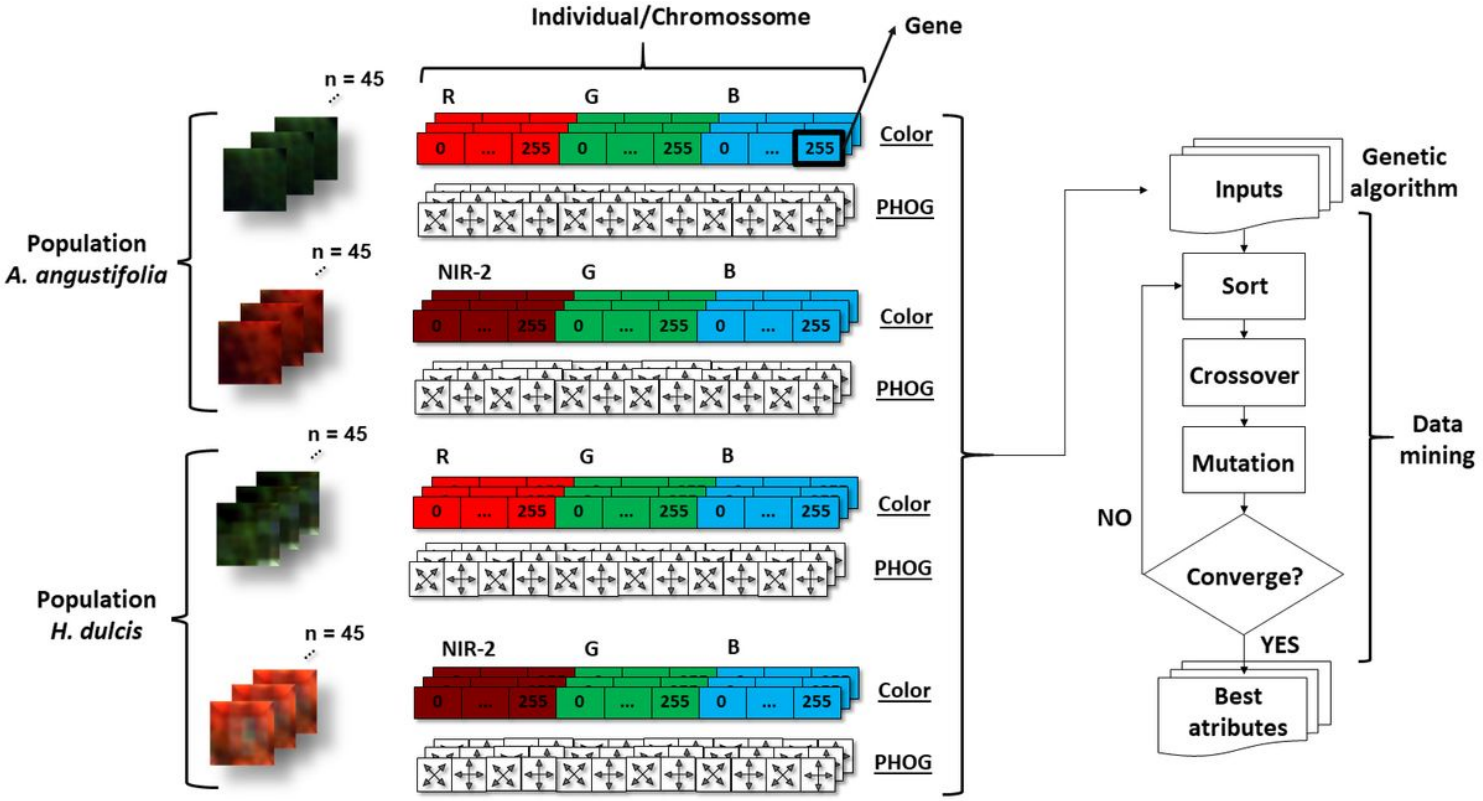

Figure 4

Scheme of the mining process of color attributes and PHOG by Genetic Algorithm – GA. Legend: Scheme of color and texture attributes (PHOG) for each RGB and NIR composition, and for each species A. angustifolia and H. dulcis, to be selected by GA algorithm.

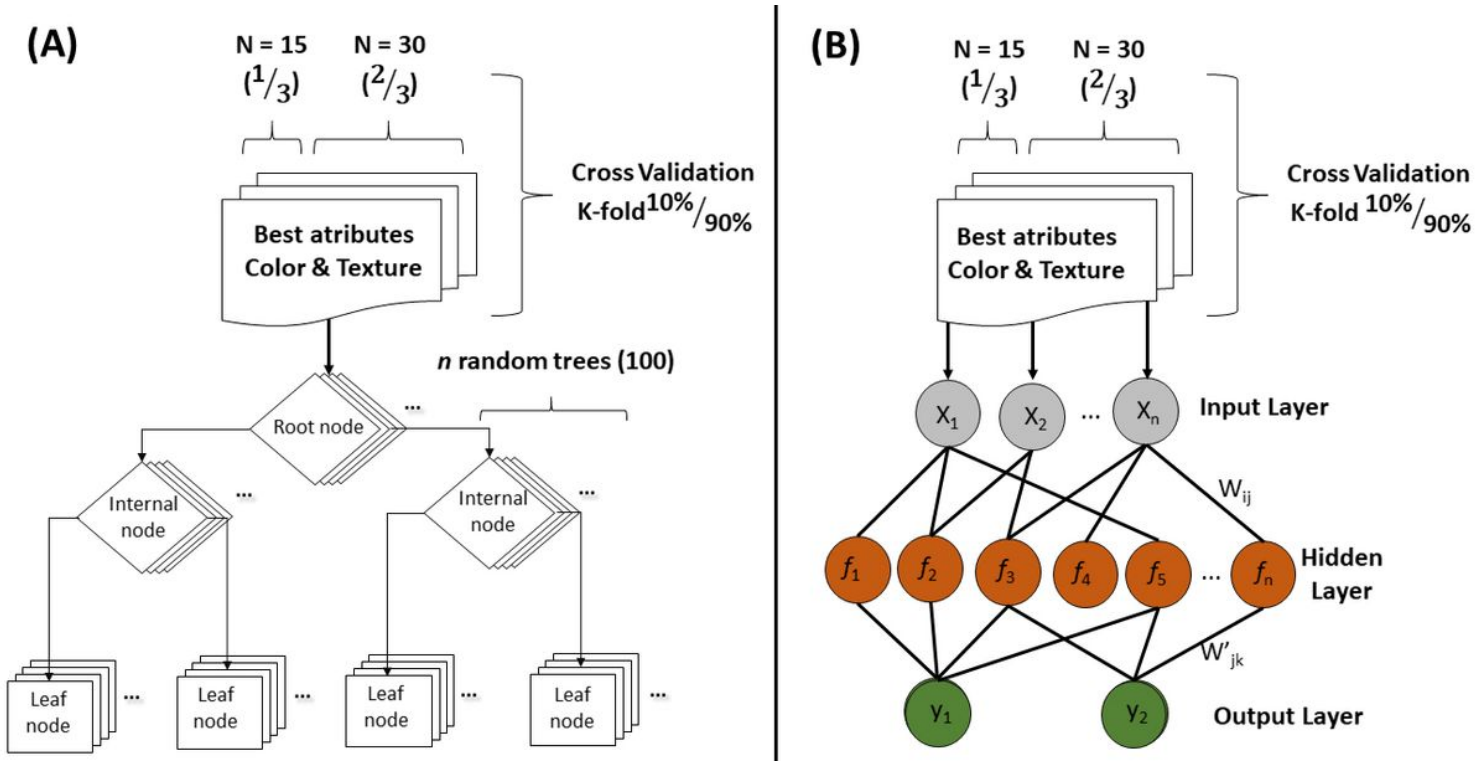

Figure 5

Random Forest (RF) and Artificial Neural Network Multilayer Perceptron (ANN-MLP) Architecture. Legend: (A) representation of the classification process performed by RF, (B) representation of neural network architecture in perceptron layers. It can be noted that the attribute entry for both classifiers was previously selected by the GA and presented a division of 2/3 of attributes for model training and 1/3 for external validation.

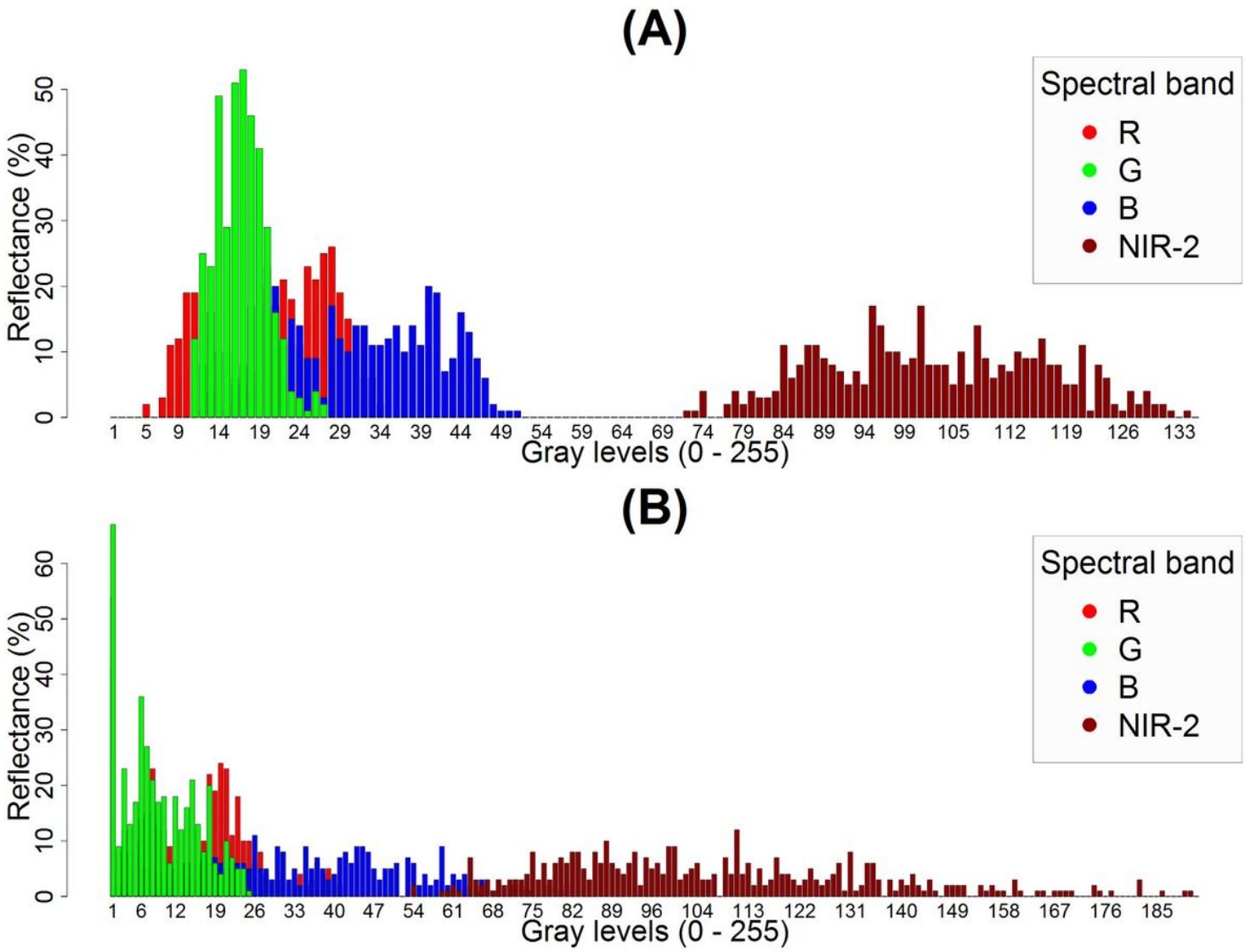

Figure 6

Reflectance distribution histograms of the selected bands for each species A. angustifolia and H. dulcis. Legend: (A) Histogram of distribution of reflectance values for the four bands selected in the work for A. angustifolia. (B) Histogram for H. dulcis. Reflectance percentage values range from 0 to 100% and gray levels in 8 bits from 0 (white) to 255 (black). The axes were limited to the maximum values for easy visualization.

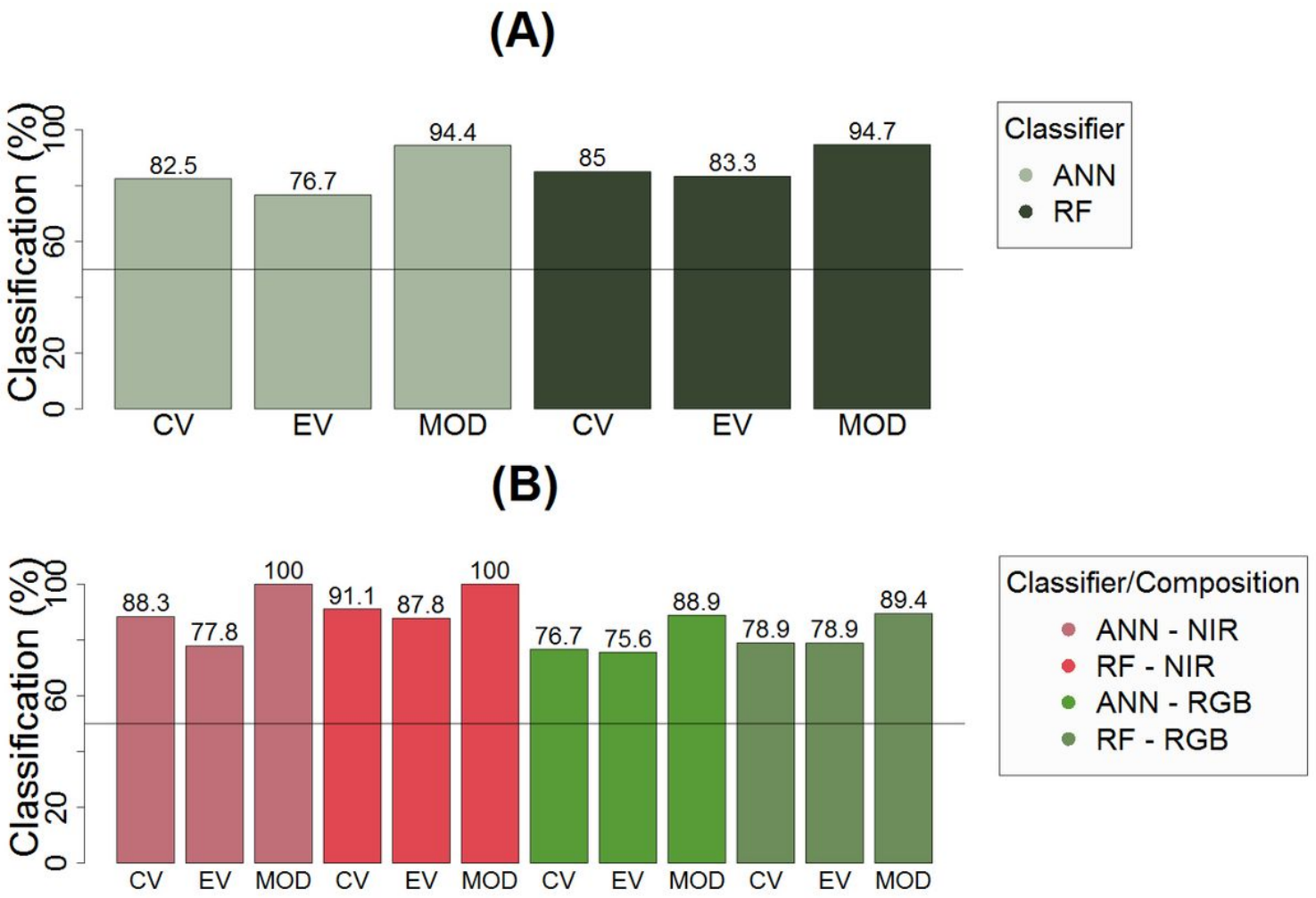

Figure 7

Classifications percentage by ANN and RF algorithm (without distinction of color and texture attributes) (A) and considering both color and texture descriptors for each classifier (B). Legend: (A) Average classifications by ANN and RF (regardless of composition). (B) Average classifications by ANN and RF taking into account the composition RGB and NIR. The black line parallel to the horizontal axis represents 50% of classification. The meaning of the acronyms is CV Cross-validation, EV External Validation and MOD classification using all instances.

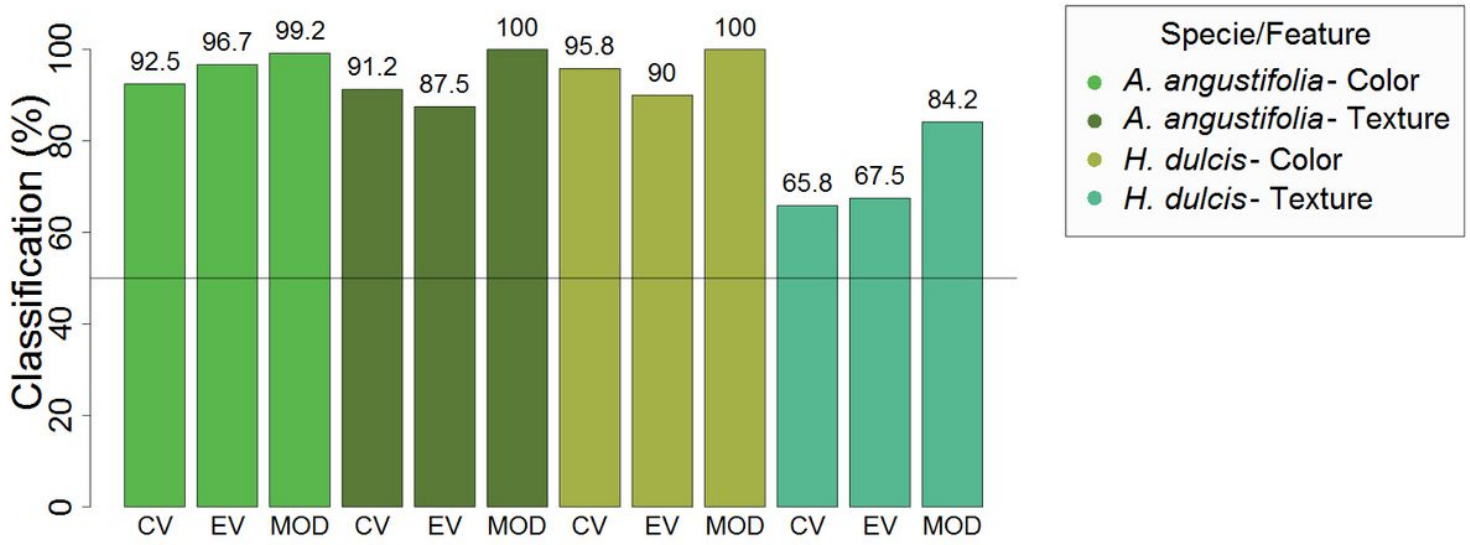

Figure 8

Classifications percentage by species and descriptors (color and texture), regardless of classifier (RF and ANN). Legend: The black line parallel to the horizontal axis represents 50% of classification. The meaning of the acronyms is CV Cross-validation, EV External Validation and MOD classification using all instances.

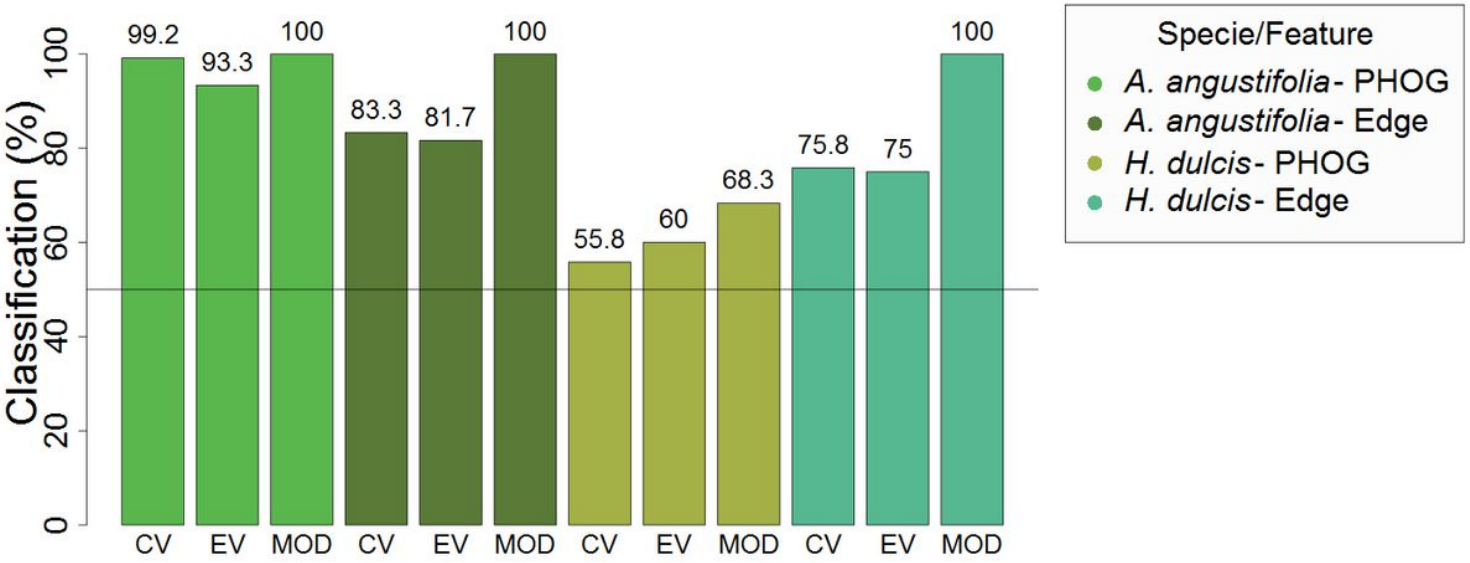

Figure 9

Classifications percentage by species and texture descriptors, regardless of classifier (RF and ANN). Legend: The black line parallel to the horizontal axis represents 50% of classification. The meaning of the acronyms is CV Cross-validation, EV External Validation and MOD classification using all instances.

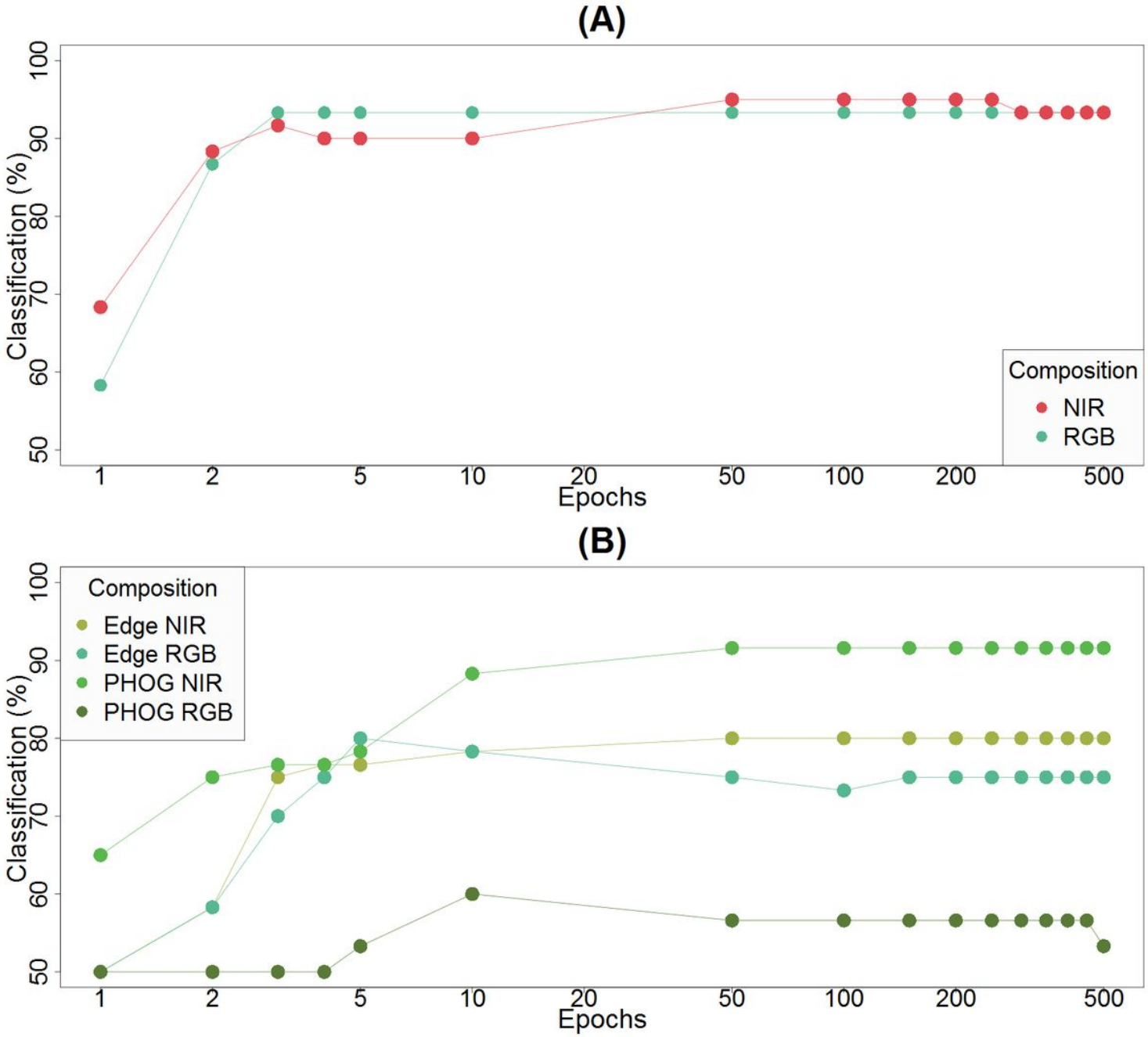

Figure 10

ANN learning ratio as a function of epochs for each composition and descriptor. Legend: (A) Percentage of classification as a function of the number of epochs for the color attributes (RGB and NIR). (B) Percentage of classification as a function of the number of epochs for the texture attributes (PHOG and Edge Filter).